Biomedicine & Pharmacotherapy 176 (2024) 116901

Contents lists available at ScienceDirect

Biomedicine & Pharmacotherapy

journal homepage: www.elsevier.com/locate/biopha

Protective effects of *Amauroderma rugosum* on dextran sulfate sodium-induced ulcerative colitis through the regulation of macrophage polarization and suppression of oxidative stress

Jingjing Li [a,f,1], Xi Luo [b,1], Polly Ho-Ting Shiu [c,1], Yanfen Cheng [b], Xin Nie [d], Panthakarn Rangsinth [c], Benson Wui Man Lau [a], Chengwen Zheng [c], Xuebo Li [b], Renkai Li [c], Simon Ming-Yuen Lee [e], Chaomei Fu [b], Sai-Wang Seto [e,f,*], Jinming Zhang [b,**], George Pak-Heng Leung [c,***]

[a] *Department of Rehabilitation Sciences, Faculty of Health and Social Sciences, Hong Kong Polytechnic University, Hung Hom, Kowloon, Hong Kong SAR, China*
[b] *State Key Laboratory of Southwestern Chinese Medicine Resources, School of Pharmacy, Chengdu University of Traditional Chinese Medicine, Chengdu, China*
[c] *Department of Pharmacology and Pharmacy, Li Ka Shing Faculty of Medicine, The University of Hong Kong, Hong Kong SAR, China*
[d] *State Key Laboratory of Quality Research in Chinese Medicine and Institute of Chinese Medical Sciences, University of Macau, Macao SAR, China*
[e] *Department of Food Science and Nutrition, Faculty of Science, Hong Kong Polytechnic University, Hung Hom, Kowloon, Hong Kong SAR, China*
[f] *The Research Centre for Chinese Medicine Innovation, Hong Kong Polytechnic University, Hung Hom, Kowloon, Hong Kong SAR, China*

ARTICLE INFO

Keywords:
Amauroderma rugosum
Ulcerative colitis
Macrophage polarization
oxidative stress

ABSTRACT

Background: Amauroderma rugosum (AR) is a medicinal mushroom commonly used to treat inflammation, gastric disorders, epilepsy, and cancers due to its remarkable anti-inflammatory and anti-oxidative properties. This study was designed to evaluate the pharmacological effects of AR and its underlying mechanism of action against ulcerative colitis (UC) *in vitro* and *in vivo*.

Methods: A UC mouse model was established by administration of dextran sulfate sodium (DSS). AR extract was administered intragastrically to mice for 7 days. At the end of the experiment, histopathology, macrophage phenotype, oxidative stress, and inflammatory status were examined *in vivo*. Furthermore, RAW 264.7, THP-1, and Caco-2 cells were used to elucidate the mechanism of action of AR *in vitro*.

Results: AR extract (0.5–2 mg/mL) significantly suppressed lipopolysaccharide (LPS) and interferon-gamma (IFN-γ)-induced M1 macrophage (pro-inflammatory) polarization in both RAW 264.7 and THP-1 cells. LPS-induced pro-inflammatory mediators (nitric oxide, TNF-α, IL-1β, MCP-1, and IL-6) were reduced by AR extract in a concentration-dependent manner. Similarly, AR extract downregulated MAPK signaling activity in LPS-stimulated RAW 264.7 cells. AR extract elicited a concentration-dependent increase in the mRNA expression of M2 (anti-inflammatory) phenotype markers (CD206, Arg-1, Fizz-1, and Ym-1) in RAW 264.7 cells. Moreover, AR extract suppressed DSS-induced ROS generation and mitochondrial dysfunction in Caco-2 cells. The *in vivo*

Abbreviations: 6-OHDA, 6-Hydroxydopamine; AR, *Amauroderma rugosum*; Arg-1, Arginase-1; CAT, Catalase; DSS, Dextran sulfate sodium; DAI, Disease activity index; DHE, Dihydroethidium; ERK, Extracellular signal-regulated kinase; FFAR4, Free fatty acid receptor 4; GO, Gene ontology; GSH, Glutathione; H&E, Hematoxylin and eosin; HIF-1α, Hypoxia-inducible factor-1α; IFN-γ, Interferon-γ; IL, Interleukin; INOS, Inducible nitric oxide synthase; JNK, c-Jun N-terminal kinase; KEGG, Kyoto encyclopedia of genes and genomes; LPS, Lipopolysaccharide; MAPK, Mitogen-activated protein kinase; MCP-1, Monocyte chemoattractant protein-1; MDA, Malondialdehyde; MTORC, Mammalian target of rapamycin complex; NO, Nitric oxide; NLPR3, NOD-like receptor protein 3; PAS, Periodic acid-Schiff; PPARγ, Peroxisome proliferator-activated receptor γ; PPI, Protein-protein interaction; ROS, Reactive oxygen species; SOD, Superoxide dismutase; STAT3, Signal transducer and activator of transcription 3; TAMs, Tumor-associated macrophages; TNF-α, Tumor necrosis factor-α; UC, Ulcerative colitis.

* Correspondence to: Department of Food Science and Nutrition, The Hong Kong Polytechnic University, Room Y851, Hung Hom, Kowloon, Hong Kong SAR, China.

** Correspondence to: State Key Laboratory of Southwestern Chinese Medicine Resources, College of Pharmacy, Chengdu University of Traditional Chinese Medicine, No.1166 Liutai Avenue, Wenjiang District, Chengdu city, Chengdu, China.

*** Correspondence to: Li Ka Shing Faculty of Medicine, Laboratory Block, Faculty of Medicine Buliding, Department of Pharmacology and Pharmacy, University of Hong Kong, 2/F, 21 Sassoon Road, Hong Kong SAR, China.

E-mail addresses: saiwang.seto@polyu.edu.hk (S.-W. Seto), cdutcmzjm@126.com (J. Zhang), gphleung@hku.hk (G.P.-H. Leung).

[1] These authors contributed equally to the paper

https://doi.org/10.1016/j.biopha.2024.116901
Received 28 February 2024; Received in revised form 30 May 2024; Accepted 6 June 2024
Available online 15 June 2024

experiment revealed that AR extract (200 mg/kg) increased colon length compared to the DSS-treated group. In addition, disease activity index, spleen ratio, body weight, oxidative stress, and colonic inflammation were markedly improved by AR treatment in DSS-induced UC mice. Finally, AR suppressed M1 and promoted M2 macrophage polarization in UC mice.

Conclusion: The AR extract protected against DSS-induced UC by regulating macrophage polarization and suppressing oxidative stress. These valuable findings suggest that adequate intake of AR can prevent and/or treat UC.

1. Introduction

Ulcerative colitis (UC) is one of the most common inflammatory bowel diseases worldwide. According to recent epidemiological statistics, the annual incidence of UC in North America ranges from 8.8–23.1 per 100,000 people and is rising globally every year, particularly in newly industrialized countries[1]. The most common symptoms of UC include diarrhea, abdominal pain, rectal bleeding, fatigue, and weight loss[2]. UC is characterized by recurring and alternating episodes of mucosal inflammation. The disease typically initiates in the rectum and spreads continuously through the colon[3]. If left untreated, the persistent inflammatory response of UC can lead to ongoing bowel damage and increase the probability of hospitalizations, surgeries, and colorectal cancer[4]. Therefore, it is imperative to find more effective and more promising drugs for the treatment of UC.

UC is a complex disease that can be categorized as a dysregulation of the immune system caused by a complex interplay of genetically inherited genes and environmental stimuli that ultimately triggers chronic intestinal inflammation[2]. Although the exact pathological mechanism of UC remains elusive, scientists believe that the imbalance of M1/M2 macrophages plays a vital role in the development of UC[5]. Generally, macrophages can be classified as M1 and M2 macrophages. M1 macrophages are usually polarized by interferon-gamma (IFN-γ) and/or lipopolysaccharides (LPS), contributing to a pro-inflammatory response[6]. In contrast, M2 macrophages are stimulated by interleukin (IL)-4 and/or IL-13, and they perform immunosuppressive functions[6]. Numerous studies have shown that the imbalance of macrophage polarization contributes to the pathogenesis of UC[7–9]. Abnormal conditions, such as genetic mutations or environmental factors, can induce the imbalance of M1 or M2 macrophage polarization in the colon[10]. Excessive M1 macrophage polarization and insufficient M2 macrophage polarization can lead to an imbalance in the regulation of colon inflammation, ultimately transforming a physiological inflammatory response into pathological colon damage[11]. Shifting the macrophages from the M1 to the M2 phenotype is considered an effective strategy for the treatment of UC because M2 macrophages can release various anti-inflammatory chemokines and cytokines to suppress the inflammatory response, thereby protecting the colon cells from inflammation-induced damage[12]. Therefore, targeting macrophages and converting them from M1 to M2 is a promising strategy for the prevention and/or treatment of UC.

Amauroderma rugosum (AR) is an herb traditionally used in Chinese medicine as a common treatment for inflammation, gastric disorders, epilepsy, and cancers in China and Malaysia[13]. It is commonly used as a dietary mushroom and belongs to a genus of basidiomycete in the family Ganodermataceae. Although the pharmacological properties of AR have rarely been studied, we previously reported that the extract of AR produces remarkable anti-oxidative effects in neuronal cells and cardiomyocytes. We subsequently demonstrated that AR extract can protect PC12 cells against 6-OHDA-induced neurotoxicity by inhibiting oxidative stress and apoptosis[14]. Additionally, the anti-inflammatory properties of AR have been demonstrated by other studies[15–17]. However, there is no evidence to support the use of AR for the treatment of UC. Based on its remarkable anti-inflammatory and ani-oxidative effects, we hypothesized that AR extract also may be effective in preventing and/or treating UC. Hence, this study investigated the protective effects of AR extract against dextran sulfate sodium (DSS)-induced UC and further explored the underlying mechanism of action of AR.

2. Materials and methods

Materials and methods are moved to the supplementary file.

3. Results

3.1. Chemical analysis of AR extract

We employed chemical assays to determine that the total amounts of polysaccharides, triterpenes, phenolic compounds, and proteins in AR extract were 42.45 ± 2.88 mg glucose/g, 6.10 ± 0.02 mg oleanolic acid/g, 6.60 ± 0.13 mg gallic acid/g, and 212.01 ± 8.29 mg bovine serum albumin/g, respectively (**Table 2, supplementary file**). Additionally, the major components of the AR extract according to our previous report, ganoderic acid A, ganoderic acid G, lucidenic acid A, and ergosterol, were quantified using HPLC analysis (Fig. S1). The average amounts of ganoderic acid A, ganoderic acid G, lucidenic acid A, and ergosterol in the AR extract were 9.39 μg/g, 12.20 μg/g, 15.69 μg/g, and 1477.68 μg/g, respectively (**Table 3, supplementary file**).

3.2. Network pharmacology analysis of AR for treating UC

To predict the potential mechanisms of AR in the treatment of UC, we performed a network pharmacology analysis. First, the potential proteins that could be affected by AR were predicted by TCMSP and BATMAN-TCM databases. Then these targets were selected and imported into STRING database for the further PPI network analysis (Fig. 1**A**). Eventually, a total number of 45 overlapping proteins between AR-associated and UC-associated proteins were identified, including STAT3, NLRP3, and NF-κb. These are the key proteins contribute to the development of UC, and they could be considered as the potential therapeutic targets for the treatment of UC. Next, GO/KEGG analysis was performed based on DAVID database to explore the biological functions of these 45 overlapping proteins. The results of KEGG analysis revealed the top 16 significantly enriched signaling pathways, including MAPK signaling pathway, JAK-STAT signaling pathway, as well as the pathways involved in inflammatory bowel disease (Fig. 1**B**). Subsequently, the top 20 significantly enriched terms in molecular function, cellular component, and biological process categories from GO enrichment analysis were analyzed and displayed in Fig. 1**C**. The results indicated that the above-mentioned overlapping proteins might be involved in the different biological process, such as inflammatory responses, signal transduction, and regulation of oxidative stress, etc. Eventually, the relationships between the major constituents, potential targets, and potential signaling pathways involved in AR-induced protective effects against UC were constructed by Cytoscape 3.7.1 software (Fig. 1**D**).

3.3. AR suppressed M1 macrophage polarization in vitro

First, we examined the cytotoxicity of AR water extract in RAW 264.7 and THP-1 cells using MTT assays. The results indicated that AR

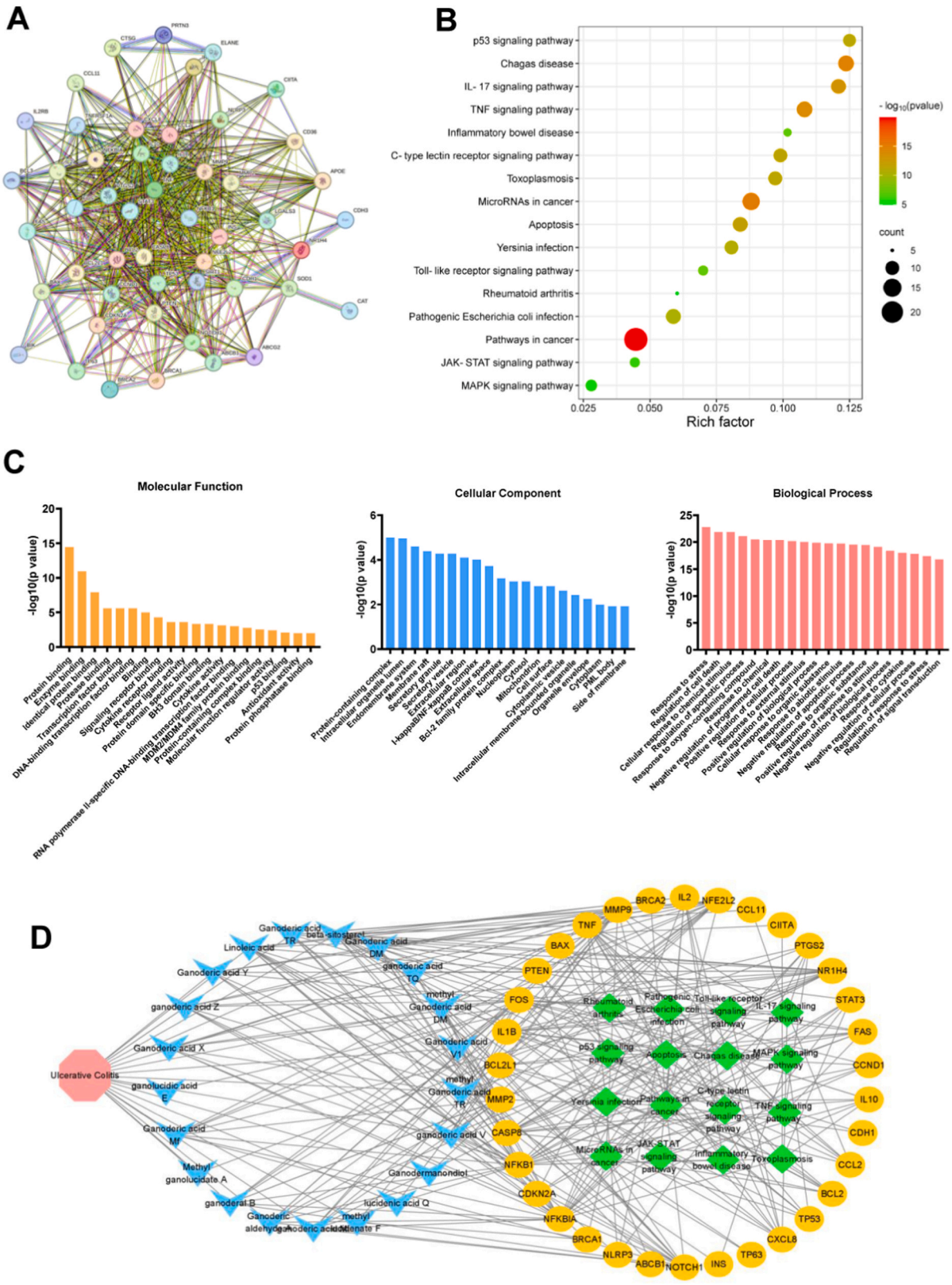

Fig. 1. Network pharmacology analysis of AR-associated proteins for treating UC. (A) Protein-protein interaction (PPI) analysis was used to detect different targets in AR treatment of UC. **(B)** Kyoto encyclopedia of genes and genomes (KEGG) analysis was used to predict the potential signaling pathways involved in AR treatment of UC. **(C)** Gene ontology (GO) enrichment analysis of the predicted proteins in AR treatment of UC, including biological process, molecular function, and cellular component. **(D)** Compound-target-pathway-disease analysis in AR treatment of UC. Pink hexagon: UC; blue triangle: the major compounds of AR; orange oval: the potential targets, and the green quads represents KEGG pathway.

(0–20 mg/mL) was safe for both cell types (Fig. S2A **and B)**. CD86 is one of the typical surface biomarkers used for detecting M1 macrophages. Here, we detected the expression of CD86 in RAW 264.7 and THP-1 cells using flow cytometry. RAW 264.7 cells and THP-1 cells were significantly polarized into M1-like macrophages in the presence of LPS (20 ng/mL) plus IFN-γ (20 ng/mL), as evidenced by the increased expression of CD86 (Fig. 2**A and B)**. By contrast, AR (2 mg/mL) treatment did not affect CD86 expression in either RAW 264.7 or THP-1 cells. The ratio of CD86-positive cells in LPS + IFN-γ-treated RAW 264.7 and THP-1 cells increased by 103 % and 54 %, respectively (Fig. 2**C and D)**. However, the enhanced CD86 expression could be dose-dependently inhibited by AR (Fig. 2**C and D)**, suggesting that AR extract can inhibit M1 macrophage polarization.

Common biomarkers of M1 macrophages include inducible nitric oxide synthase (iNOS), tumor necrosis factor-α (TNF-α), IL-6, and IL-1β. Next, we investigated the mRNA expression of these biomarkers in RAW 264.7 cells to further confirm AR's inhibitory effects on M1 macrophage polarization. Similar to the results above, LPS + IFN-γ treatment strongly elevated mRNA expression of iNOS, TNF-α, IL-6, and IL-1β in RAW 264.7 cells, whereas AR extract did not affect such mRNA expression. AR suppressed mRNA expression of iNOS, TNF-α, IL-6, and IL-1β in a dose-dependent manner at concentration ranging from 0.5–2 mg/mL. As compared to the LPS + IFN-γ group, mRNA expression of iNOS, TNF-α, IL-6, and IL-1β in 2 mg/mL AR-treated RAW 264.7 cells were strongly decreased 6.7-fold, 15.2-fold, 11.5-fold, and 26.5-fold, respectively (Fig. 2**E–H)**. In line with the results of mRNA expression, LPS + IFN-γ treatment significantly increased the protein expression of iNOS in RAW 264.7 cells (Fig. 2**I)**, while such an increase in iNOS was reduced by 72 % and 89 % in response to 1 mg/mL and 2 mg/mL AR treatment, respectively (Fig. 2**J)**. Collectively, these findings suggested a potential effect of AR extract on the inhibition of M1 macrophage polarization.

3.4. AR suppressed inflammation response and MAPK signaling pathway

The release of inflammation-related cytokines, including TNF-α, IL-6, IL-1β, nitric oxide (NO), and monocyte chemoattractant protein-1 (MCP-1), was determined in the culture medium of LPS-treated RAW 264.7 cells using ELISA kits. LPS treatment significantly stimulated the release of TNF-α, IL-6, IL-1β, NO, and MCP-1 compared to untreated cells, whereas no obvious changes were detected in the AR treatment group (Fig. 3**A–E)**. The levels of TNF-α, IL-6, IL-1β, NO, and MCP-1 increased approximately 63.5-fold, 3.3-fold, 3.5-fold, 2.4-fold, and 16.3-fold, respectively, in response to LPS treatment. However, AR extract dose-dependently suppressed the LPS-stimulated release of these pro-inflammatory cytokines. Specifically, 2 mg/mL AR sharply reduced the level of TNF-α, IL-6, IL-1β, NO, and MCP-1 by 45 %, 57 %, 48 %, 94 %, and 75 %, respectively, compared to LPS-treated cells (Fig. 3**A–E)**.

The mitogen-activated protein kinase (MAPK) signaling pathway plays an essential role in the regulation of the inflammatory response. The expression levels of proteins involved in the MAPK signaling pathway, including p-MEK1/2, p-ERK1/2, p-JNK1/2, and p-p38, were examined by western blot assay (Fig. 3**G)**. LPS triggered significant phosphorylation of MEK1/2, ERK1/2, JNK1/2, and p38 compared to untreated RAW 264.7 cells, while AR treatment did not affect the phosphorylation of these proteins (Fig. 3**G)**. Notably, AR treatment inhibited the phosphorylation of MEK1/2, ERK1/2, JNK1/2, and p38 in LPS-treated RAW 264.7 cells without affecting their total protein expressions (Fig. 3**G)**. Importantly, 2 mg/mL AR remarkably decreased the ratios of p-MEK1/2 to MEK1/2 (Fig. 3**F)**, p-ERK1/2 to ERK1/2 (Fig. 3**H)**, p-JNK1/2 to JNK1/2 (Fig. 3**I)**, and p-p38 to p38 (Fig. 3**J)** by 60 %, 90 %, 288 %, and 249 %, respectively. Collectively, these results demonstrated that AR extract significantly suppressed LPS-induced inflammation and MAKP signal transduction.

3.5. AR promoted M2 macrophage polarization in vitro

The effect of AR extract on the polarization of M2 macrophages was further investigated in RAW 264.7 cells and THP-1 cells (Fig. 4**A and B)**. Cells treated with IL-4 and IL-13 served as positive controls. IL-4 + IL-13 treatment strongly polarized RAW 264.7 and THP-1 cells into M2-like macrophages, as evidenced by the enhanced expression of genes typical of M2 macrophages, including CD206, Arg-1, Fizz-1, and Ym-1 (Fig. 4**E–H)**. Similarly, AR extract significantly shifted the polarization of RAW 264.7 cells and THP-1 cells toward M2-like macrophages. AR extract dose-dependently increased the expression of the M2 macrophage surface biomarker CD206 in RAW 264.7 and THP-1 cells (Fig. 4**A and B)**. The percentage of CD206-positive RAW 264.7 and THP-1 cells increased by 49.2 % and 45.5 %, respectively, in response to 2 mg/mL AR treatment (Fig. 4**C and D)**. Moreover, AR extract significantly increased mRNA expression of CD206, Arg-1, Fizz-1, and Ym-1 in RAW 264.7 cells (Fig. 4**E–H)**. Furthermore, the effects of AR on STAT3 expressions were examined by western blot assay (Fig. 4**I).** AR extract dose-dependent elevated the expression levels of phosphor-STAT3 in RAW 264.7 cells without affecting the total amount of STAT3 (Fig. 4**J)**. This result is consistent with IL-4+IL-13 treatment. Collectively, these findings suggested that AR extract could stimulate M2 macrophage polarization *in vitro* possibly through the activation of STAT3 signaling pathway.

3.6. AR suppressed DSS-induced ROS generation and mitochondrial dysfunction in Caco-2 cells

DSS-induced oxidative stress and mitochondrial dysfunction in colon cells are the major causes of UC. Therefore, the role of AR in the prevention of DSS-induced reactive oxygen species (ROS) generation and mitochondrial dysfunction was examined in Caco-2 human colon cancer cells. AR extract was safe for Caco-2 cells at concentrations ranging from 0.5–2 mg/mL (Fig. S2 **C)** and did not cause ROS production (Fig. 5**A and B).** By contrast, 5 % DSS caused abundant ROS generation in Caco-2 cells after 24 hours of incubation (Fig. 5**A and B)**. Fluorescence imaging and flow cytometry analysis showed that the ROS levels in DSS-treated Caco-2 cells increased by 156 % and 67 %, respectively (Fig. 5**D and E)**. However, AR extract dose-dependently decreased ROS generation in DSS-treated Caco-2 cells. Notably, 2 mg/mL AR significantly reduced DSS-induced ROS by 144 % and 68 %, as detected by fluorescence imaging and flow cytometry, respectively (Fig. 5**D and E)**.

Next, mitochondrial respiration function of Caco-2 cells was examined using a Seahorse metabolic analyzer. DSS strongly inhibited the oxygen consumption rate of Caco-2 cells after 24 hours of treatment (Fig. 5**C)**. Additionally, DSS significantly reduced basal respiration (Fig. 5**F)**, ATP-linked respiration (Fig. 5**G)**, maximal respiration (Fig. 5**H)**, and spare respiratory capacity (Fig. 5**I)** of Caco-2 cells by 41 %, 42 %, 55 %, and 35 %, respectively. By contrast, AR extract remarkably restored mitochondrial respiration function of DSS-treated Caco-2 cells (Fig. 5**C)**. The basal respiration, ATP-linked respiration, maximal respiration, and spare respiratory capacity in DSS-treated Caco-2 cells increased by 28 %, 31 %, 39 %, and 24 %, respectively, in response to 2 mg/mL AR extract treatment (Fig. 5**F–I)**. Consequently, these results demonstrated that AR extract served a protective function against DSS-induced oxidative stress and mitochondrial dysfunction in Caco-2 cells.

3.7. AR alleviated DSS-induced UC in mice

A DSS-induced UC mouse model was established to examine the protective effects of AR against UC *in vivo*. The experiment was performed using the methodology shown in Fig. 6**A**. We recorded key parameters, including changes in body weight, disease activity index (DAI) scores, colon length, and spleen ratio, during the investigation. By treating mice with 3 % DSS for 10 days, we successfully induced UC, as

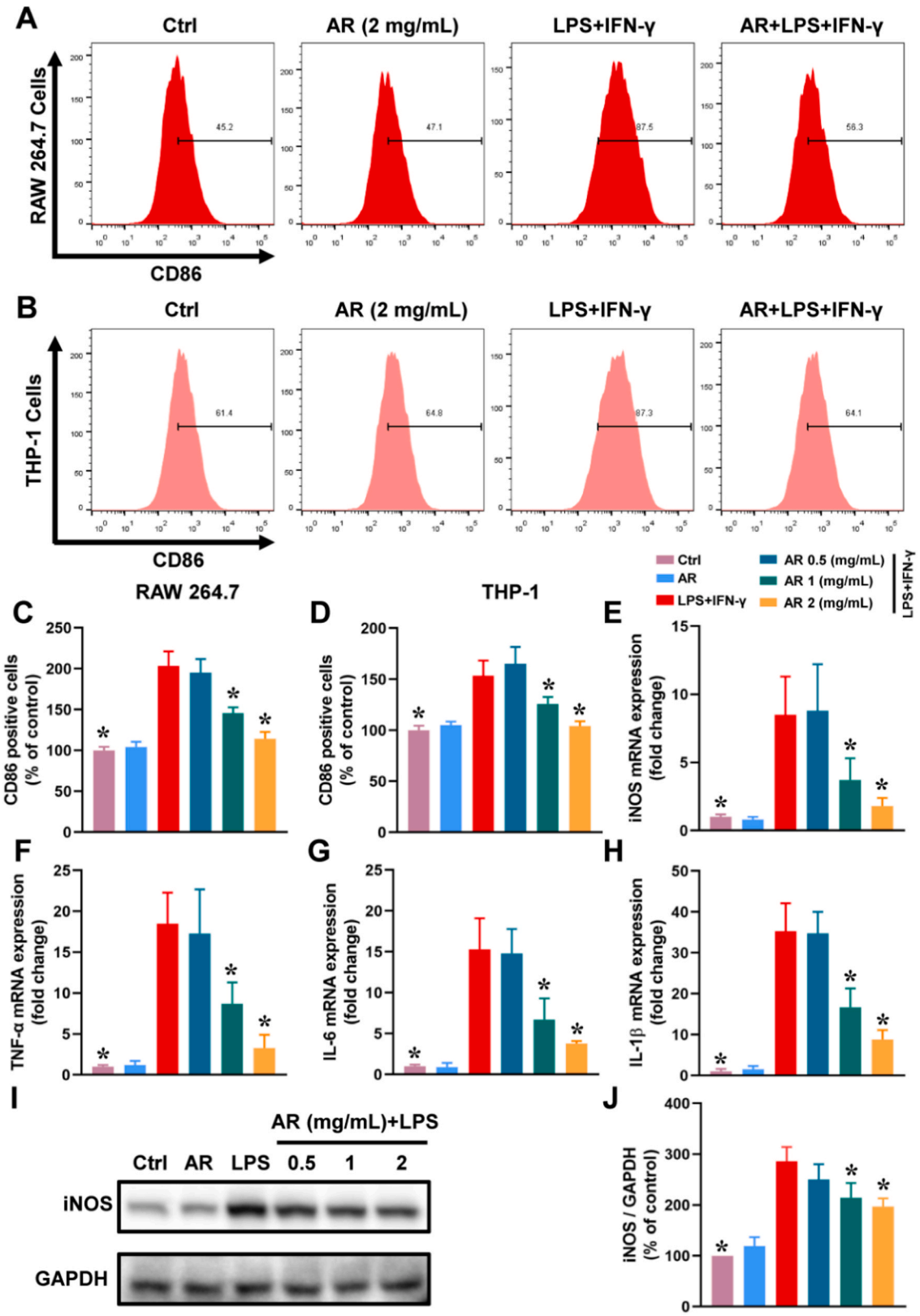

Fig. 2. AR suppresses M1 macrophage polarization *in vitro*. **(A)** RAW 264.7 cells and **(B)** THP-1 cells were treated with AR (0–2 mg/mL) in the presence or absence of LPS (20 ng/mL) plus IFN-γ (20 ng/mL) for 48 hours, and then the surface marker of M1 macrophage CD86 was examined by flow cytometry. Quantitative analysis of CD86 expression in **(C)** RAW264.7 and **(D)** THP-1 cells, respectively. mRNA expressions of **(E)** iNOS, **(F)** TNF-α, **(G)** IL-6, and **(H)** IL-1β in RAW 264.7 cells were detected by qPCR. **(I)** The protein expression of iNOS in RAW 264.7 cells was examined by western blot assay. **(J)** Quantitative analysis of iNOS in RAW 264.7 cells. Data are presented as means ± SD for three independent trials. *p <0.05 versus LPS+IFN-γ group. One-way ANOVA followed by Tukey's test was used.

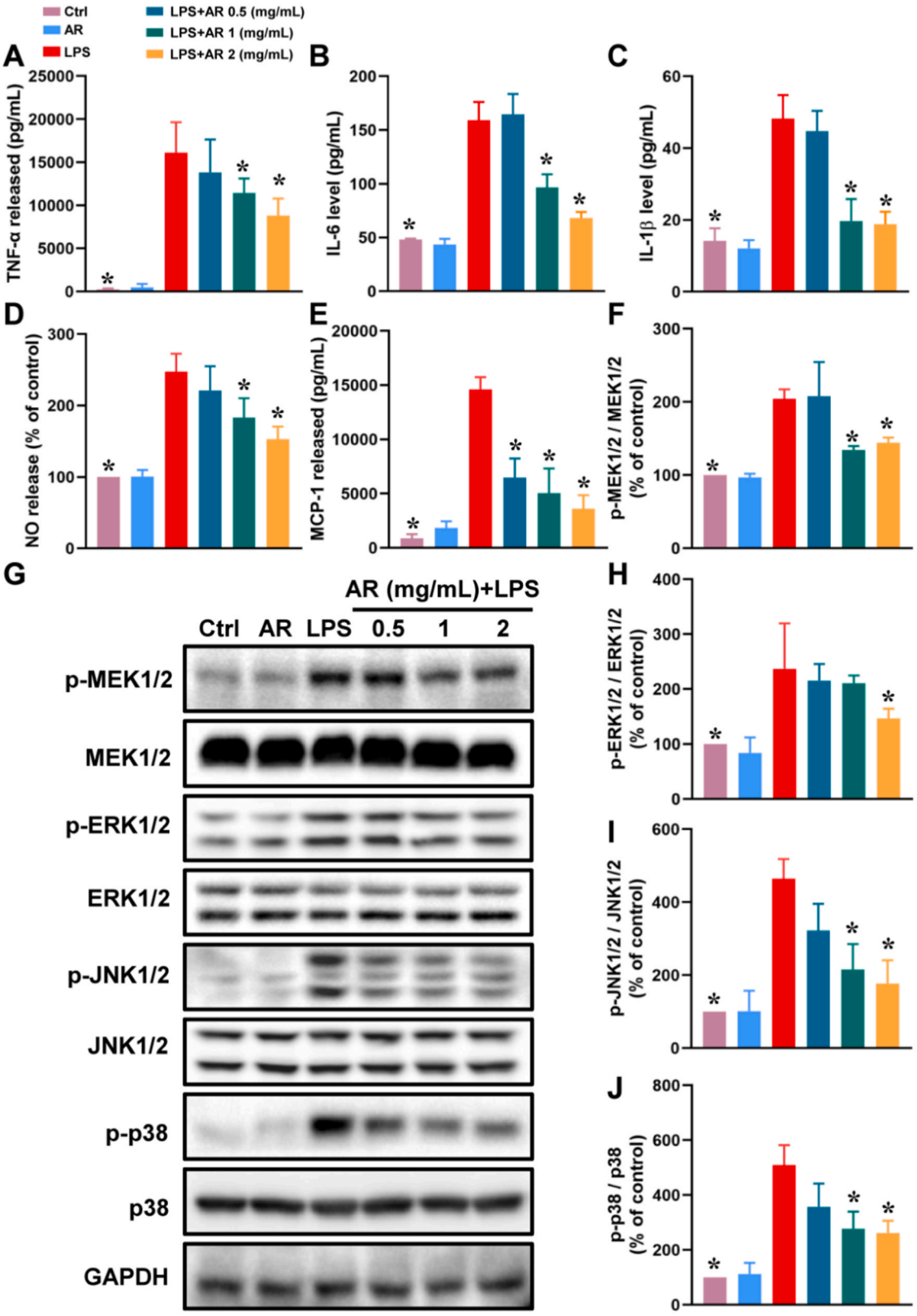

Fig. 3. AR suppresses the release of pro-inflammatory cytokines and down-regulates MAPK signaling pathway. RAW 264.7 cells were treated with AR (0–2 mg/mL) in the presence or absence of LPS (100 ng/mL) plus IFN-γ (20 ng/mL) for 48 hours, and the level of **(A)** TNF-α, **(B)** IL-6, **(C)** IL-1β, **(D)** NO, and **(E)** MCP-1 in the culture medium was examined by ELISA assay. **(G)** The expression of proteins involved in MAPK signaling pathway in the lysates of RAW 264.7 cells were detected by western blot assay. Quantitative analysis of the ratio of **(F)** p-MEK1/2 to MEK1/2, **(H)** ERK1/2 to ERK1/2, **(I)** JNK1/2 to JNK1/2, **(J)** p-p38 to p38 in RAW 264.7 cells lysate. Data are presented as means ± SD for three independent trials. *p <0.05 versus LPS+IFN-γ group. One-way ANOVA followed by Tukey's test was used.

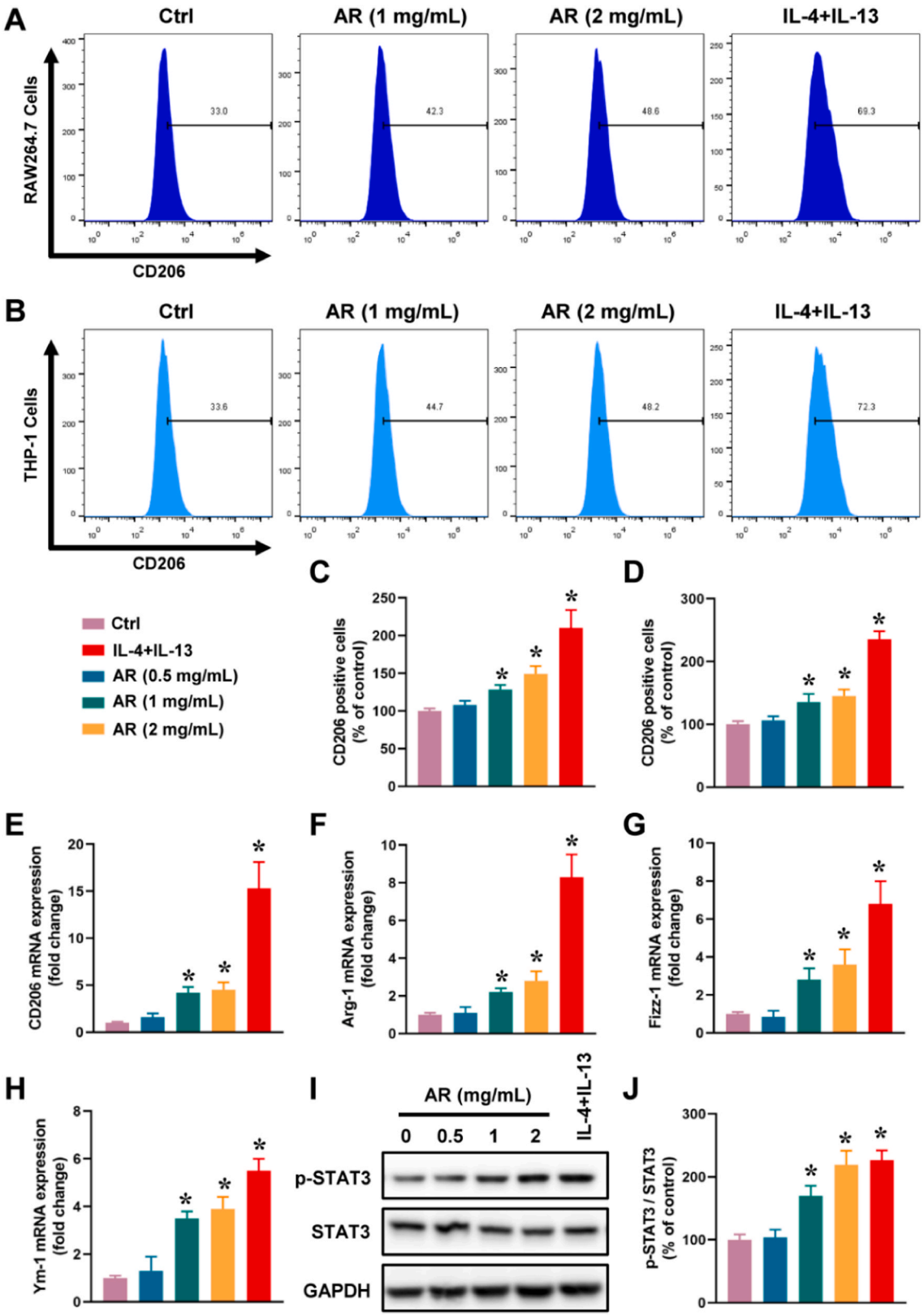

Fig. 4. AR promotes M2 macrophage polarization *in vitro*. **(A)** RAW 264.7 cells and **(B)** THP-1 cells were treated with AR (0–2 mg/mL) or IL-4 (20 ng/mL) plus IL-13 (20 ng/mL) for 48 hours, and then the surface marker of M2 macrophage CD206 was examined by flow cytometry. Quantitative analysis of CD206 expression in **(C)** RAW264.7 and **(D)** THP-1 cells, respectively. mRNA expressions of **(E)** CD206, **(F)** Arg-1, **(G)** Fizz-1, and **(H)** Ym-1 in RAW 264.7 cells were detected by qPCR. **(I)** The protein expressions of phosphor-STAT3 and STAT3 in RAW 264.7 cells were examined by western blot assay. **(J)** Quantitative analysis of the ratio of p-STAT3 to STAT3 in RAW 264.7 cells. Data are presented as means ± SD for three independent trials. *p <0.05 versus control group. One-way ANOVA followed by Tukey's test was used.

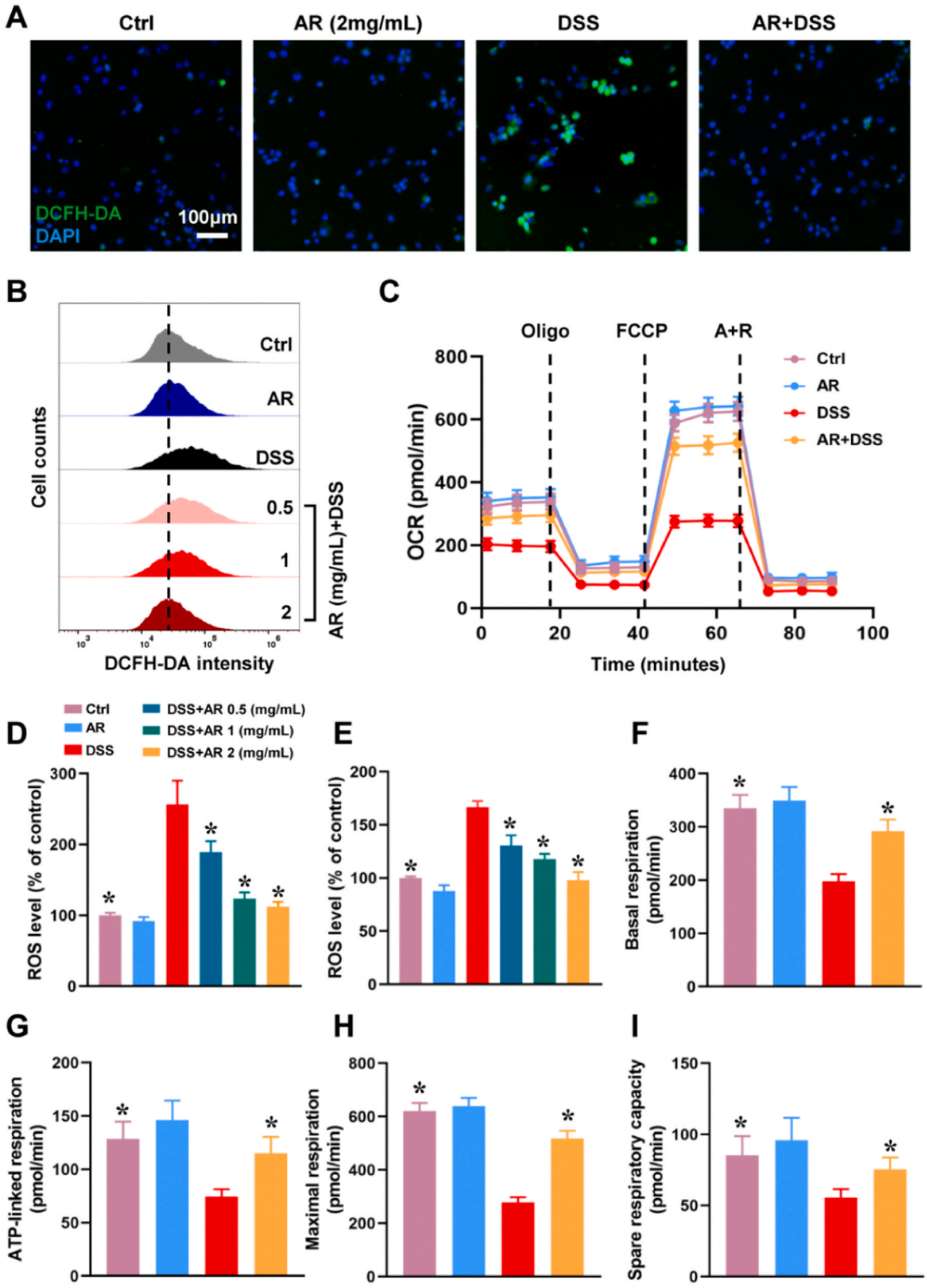

Fig. 5. AR suppresses DSS-induced ROS generation and mitochondrial dysfunction in Caco-2 cells. Caco-2 cells were treated with AR (0–2 mg/mL) in the presence or absence of 5 % DSS for 24 hours, and then the ROS generation was detected by **(A)** fluorescence microscopy and **(B)** flow cytometry before DCFH-DA labeling. **(C)** Mitochondrial respiration function of Caco-2 cells was examined by a Seahorse metabolic analyzer. Monitoring of mitochondrial oxygen consumption rate (OCR) in Caco-2 cells. Quantification of ROS levels in RAW 264.7 cells by **(D)** fluorescent imaging and **(E)** flow cytometry. Quantification of **(F)** basal respiration, **(G)** ATP-linked respiration, **(H)** maximal respiration, and **(I)** spare respiratory capacity in Caco-2 cells. Data are presented as means ± SD for three independent trials. *p <0.05 versus DSS treatment group. One-way ANOVA followed by Tukey's test was used.

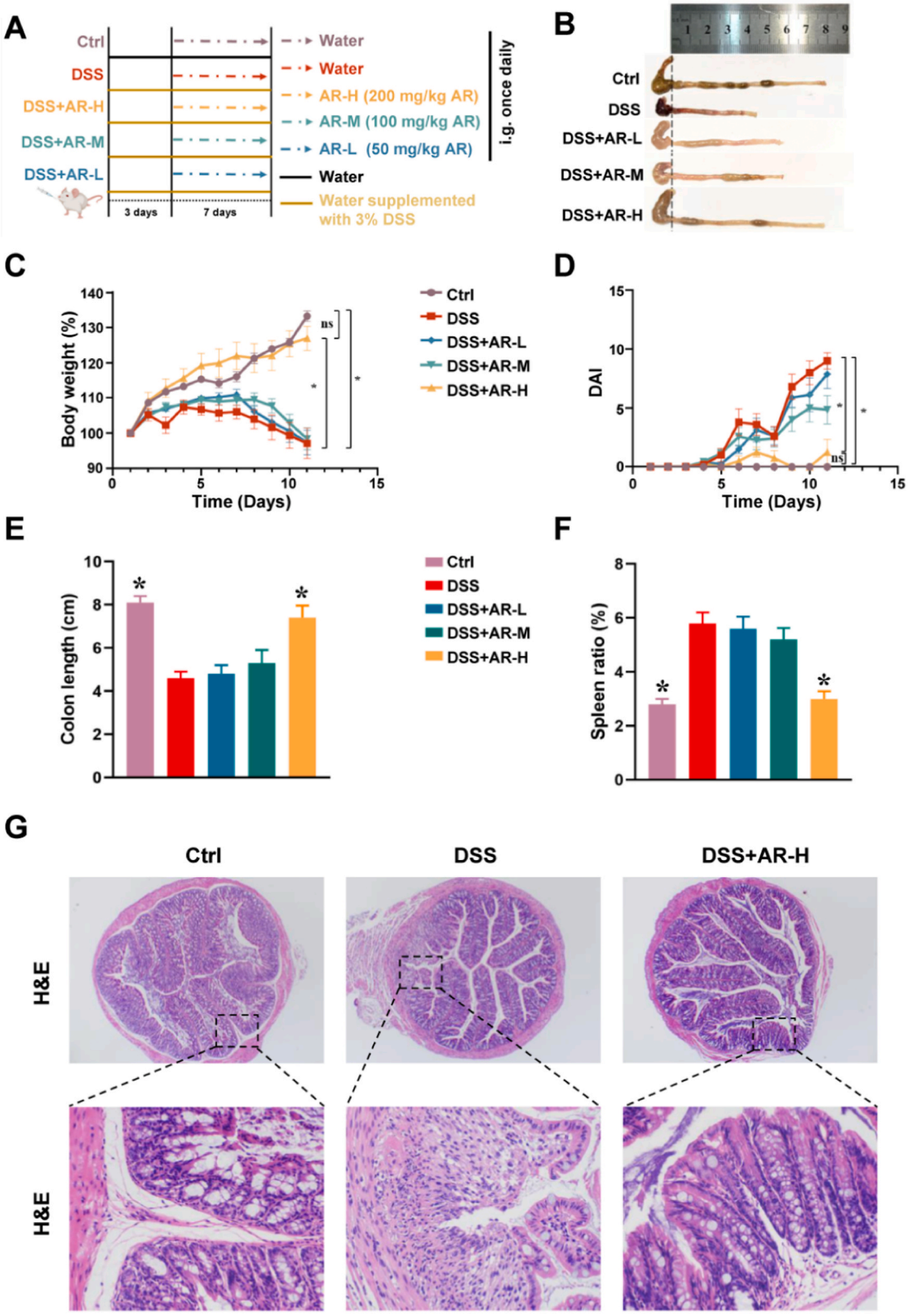

Fig. 6. AR alleviates DSS-induced ulcerative colitis in mice. (A) Schematic diagram illustrating the treatment methods of DSS-induced ulcerative colitis model in mice. **(B)** Representative images of the mouse colon tissue in each group. The changes in **(C)** body weight and **(D)** disease activity index (DAI) of the mice were monitored during the experiment. **(E)** The length of colon tissues at the end of experiments was measured and analyzed. **(F)** The spleen ratio of the mice in each group was calculated and analyzed. **(G)** H&E staining of the colon tissues. Data are presented as means ± SD for six independent trials. *p <0.05 versus DSS treatment group. One-way ANOVA followed by Tukey's test was used.

evidenced by reduced length of colon tissue (Fig. 6**B**) and body weight (Fig. 6**C**) and by increased DAI scores (Fig. 6**D**) and spleen ratio (Fig. 6**F**). Three doses of AR extract were used to examine the protective effects of AR in this model. Low (50 mg/kg) and medium (100 mg/kg) doses of AR slightly increased colon length and body weight compared to the DSS group. By contrast, a high dose (100 mg/kg) of AR significantly restored colon length and body weight in DSS-treated mice (Fig. 6**A and B**). The average colon lengths of mice after DSS treatment, the low dose of AR treatment, and the medium dose of AR treatment were 4.3 cm, 4.5 cm, and 4.9 cm, respectively. However, colon length was increased to 7.3 cm after the high dose of AR treatment (Fig. 6**E**). Moreover, the low dose of AR slightly reduced DAI scores, whereas medium and high doses of AR strongly suppressed disease activity caused by DSS (Fig. 6**D**). Additionally, DSS treatment significantly increased the spleen ratio of mice, and neither low nor medium doses of AR affected the spleen ratio. By contrast, the high dose of AR substantially suppressed the enhanced spleen ratio of DSS-treated mice (Fig. 6**F**).

Hematoxylin and eosin (H&E) staining was used to examine colonic inflammation and tissue structure in DSS-treated mice (Fig. 6**G**). The typical symptoms of colonic inflammation, including diffuse congestion, tissue edema, and mucosal adhesions, were observed in the colon tissues of DSS-treated mice. Moreover, we observed clear damage of epithelial cells and infiltration of pro-inflammatory cells in the DSS group. Nevertheless, AR (high dose) remarkably prevented colonic damage caused by DSS, as evidenced by the inhibition of tissue edema and mucosal adhesion, as well as a reduction in the numbers of damaged epithelial cells and pro-inflammatory cells (Fig. 6**G**). Periodic acid–Schiff (PAS) staining was used to label goblet cells in colon tissues. The results indicated that AR treatment could significantly prevent the loss of goblet cells in the colons of DSS-treated mice (Fig. 7**A**). Compared to the control group, the percentage of colon goblet cells decreased by 44 % in response to DSS treatment. However, the proportion of colon goblet cells increased by 33 % after AR treatment of DSS-treated mice (Fig. 7**B**). These findings suggested that AR played an important role in preventing DSS-induced UC by inhibiting colon tissue damage, restoring body weight, and blocking goblet cell loss.

3.8. AR regulated macrophage polarization in the colons of DSS-treated mice

We conducted histological analysis, including immunohistochemical staining (Fig. 7**B and C**) and immunofluorescence staining (Fig. 7**D and E**), to investigate macrophage polarization in mouse colon tissues. DSS strongly promoted the expression of iNOS and CD86 but suppressed the expression of Arg-1 and CD206 in mouse colon tissues (Fig. 7**B–E**). Compared to control group, the expression of iNOS (Fig. 7**G**) and the percentage of CD86-positive macrophages (Fig. 7**I**) in the colon tissues of DSS-treated mice significantly increased by 27 % and 19 %, respectively. By contrast, the expression of Arg-1 (Fig. 7**H**) and the percentage of CD206-positive macrophages (Fig. 7**J**) were reduced by 27 % and 9 %, respectively, in response to DSS treatment. However, AR extract substantially reduced the effects of DSS on the polarization of M1 macrophages in mouse colon tissues. AR extract sharply reduced the expression of iNOS (Fig. 7**G**) and the ratio of CD86-positive macrophages (Fig. 7**I**) by 22 % and 14 %, respectively, compared to the DSS treatment group. Moreover, the expression of Arg-1 (Fig. 7**H**) and the ratio of CD206-positive macrophages (Fig. 7**J**) in the colons of DSS-treated mice increased by 31 % and 5 %, respectively, in response to AR treatment. These findings demonstrated that DSS can shift the polarization of macrophages from M2 to M1 in mouse colons, whereas AR extract can reverse DSS-induced macrophage polarization, thereby suppressing M1 macrophage polarization and promoting M2 macrophage polarization.

3.9. AR suppressed oxidative stress and inflammation in the colons of DSS-treated mice

DSS induced severe oxidative stress in mouse colons. Dihydroethidium (DHE) staining was used to examine the accumulation of ROS (Fig. 8**A**). As expected, DSS induced abundant ROS generation in mouse colons, as evidenced by a significant increase of 39 % compared to the control group (Fig. 8**B**). Additionally, DSS increased the level of malondialdehyde (MDA) by 104 % and decreased the levels of superoxide dismutase (SOD), glutathione (GSH), and catalase (CAT) by 36 %, 58 %, and 52 %, respectively (Fig. 8**C–F**). Nevertheless, AR substantially suppressed DSS-induced oxidative stress in mouse colons. AR extract significantly reduced the levels of ROS and MDA by 36 % and 111 %, respectively, and increased SOD, GSH, and CAT levels by 27 %, 33 %, and 47 %, respectively, compared to the DSS treatment group (Fig. 8**C–F**). Additionally, AR strongly suppressed DSS-induced inflammation in mouse colons. The levels of pro-inflammatory cytokines, including IFN-γ, TNF-α, IL-6, and IL-1β, increased by 74 %, 113 %, 650 %, and 208 %, respectively, in colons of DSS-treated mice (Fig. 8**G–J**). However, the release of these cytokines could be suppressed by AR extract. AR decreased the levels of IFN-γ, TNF-α, IL-6, and IL-1β by 79 %, 98 %, 565 %, and 157 %, respectively, in the colons of DSS-treated mice (Fig. 8**C–F**). These results suggested that AR could substantially suppress DSS-induced oxidative stress and inflammation in mouse colons.

4. Discussion

The interaction between inflammation and oxidative stress plays a significant role in the pathogenesis of UC. Simultaneous inhibition of inflammation and oxidative stress is most effective in preventing and/or treating UC[18]. In this study, we demonstrated that AR extract can alleviate UC symptoms by regulating macrophage polarization and suppressing oxidative stress. AR suppressed LPS + IFN-γ-induced M1 macrophage polarization in RAW 264.7 cells by reducing the protein and mRNA expression of iNOS, TNF-α, IL-6, and IL-1β. By contrast, AR extract promoted M2 macrophage polarization in RAW 264.7 cells by increasing the mRNA expression of CD206, Arg-1, Fizz-1, and Ym-1. Moreover, AR reduced DSS-induced ROS generation and restored mitochondrial function in DSS-treated Caco-2 cells. Furthermore, AR alleviated UC development in DSS-induced UC mice by restoring body weight and colon length, inducing the conversion of M1 macrophages into M2 macrophages, and suppressing oxidative stress. These findings demonstrate the potential therapeutic efficacy of AR extract for the treatment of UC.

Notably, targeting macrophages is a potential strategy for controlling different diseases, as the imbalance of macrophage polarization is related to various diseases and inflammatory conditions[19]. In tumor microenvironment, tumor-associated macrophages (TAMs) tend to polarize into M2 macrophages and can promote tumor growth and metastasis by stimulating tumor angiogenesis and suppressing antitumor immune responses[6]. Skewing TAMs from the M2 phenotype to the M1 phenotype can effectively control tumor development and progression[20]. Previously, we demonstrated that glycyrrhetinic acid, the major component of licorice, can suppress breast cancer growth and metastasis by shifting TAMs into M1 macrophages by activating JNK1/2 signaling pathways[21]. Glycyrrhetinic acid can also suppress TAMs-induced breast cancer growth and angiogenesis[21]. Similar effects were caused by another natural product, garcinone E, one of the major bioactive compounds of *Garcinia mangostana*[22]. These findings provide valuable evidence that future drug development efforts may benefit by targeting macrophage polarization.

Additionally, converting the macrophages from the M1 to the M2 phenotype could prevent and/or treat inflammatory diseases, such as UC [19]. Clinical evidence has shown that the proportion of intestinal mucosal macrophages was significantly higher and that macrophages

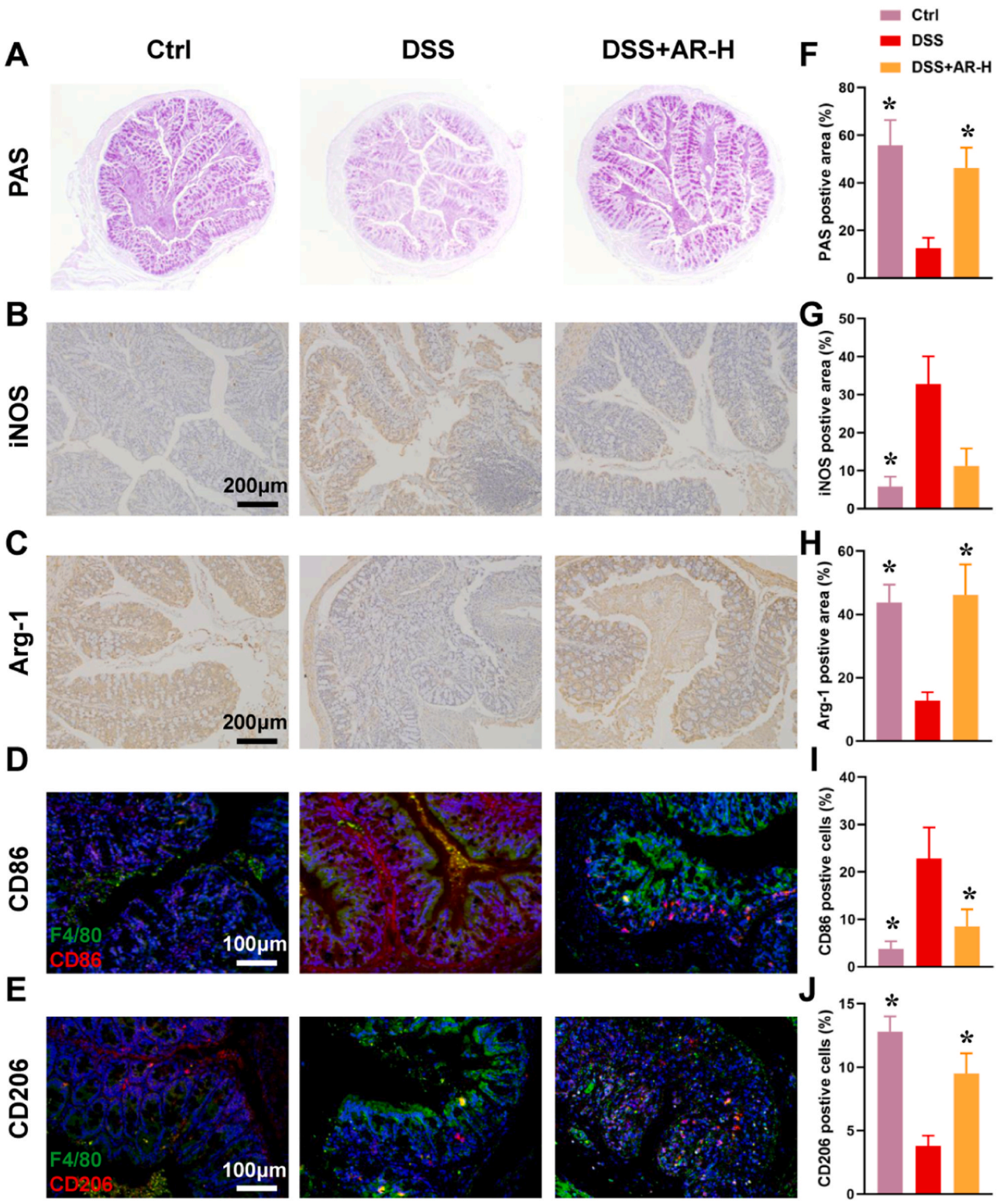

Fig. 7. AR regulates macrophage polarization in the colon of DSS-treated mice. **(A)** PAS staining of goblet cells in mouse colons. Immunohistochemical staining of **(B)** iNOS and **(C)** Arg-1 expressions in mouse colons. Immunofluorescence staining of **(D)** CD86 and **(E)** CD206 expressions in mouse colons. **(F)** Quantification of the positive PAS signals in colon tissues. Quantification of the positive signals of **(G)** iNOS and **(H)** Arg-1 in colon tissues, respectively. Quantification of the positive signals of **(I)** CD86 and F4/80 and **(J)** CD206 and F4/80 in in colon tissues, respectively. Data are presented as means ± SD for three independent trials. *p <0.05 versus DSS treatment group. One-way ANOVA followed by Tukey's test was used.

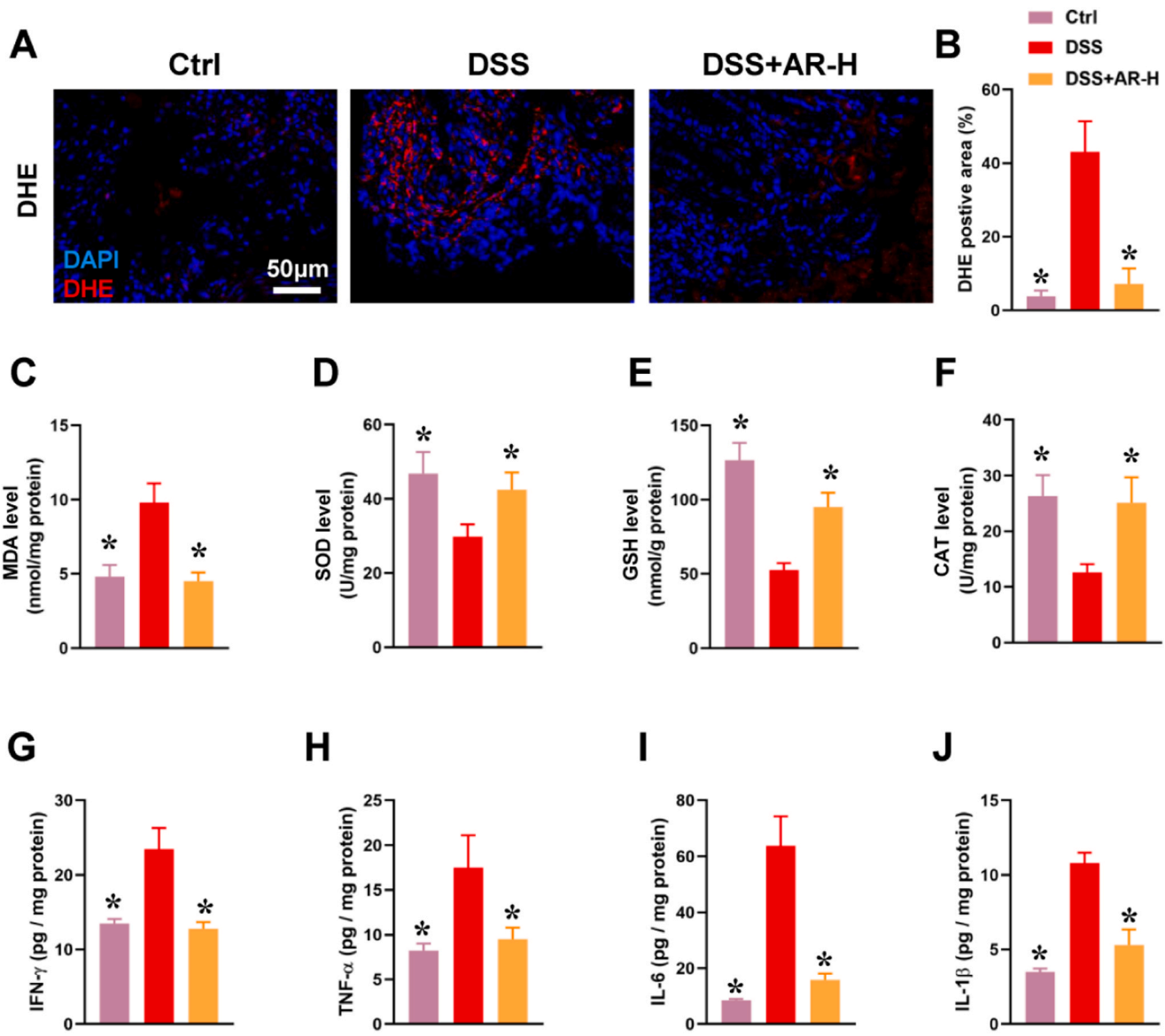

Fig. 8. AR suppresses oxidative stress and inflammation in the colon of DSS-treated mice. **(A)** DHE staining of ROS in mouse colons. **(B)** Quantification of the positive DHE signals. The levels of **(C)** MDA, **(D)** SOD, **(E)** GSH, **(F)** CAT, **(G)** IFN-γ, **(H)** TNF-α, **(I)** IL-6, and **(J)** IL-1β in the colon tissues were determined by respective ELISA assay kit. Data are presented as means ± SD for three independent trials. *p <0.05 versus DSS treatment group. One-way ANOVA followed by Tukey's test was used.

tended to be more activated in the colon tissues of UC patients compared with the lamina propria of the normal mucosa, suggesting that intestinal macrophages play an important role in the development of UC[23]. Restoring the balance of M1/M2 macrophage polarization is a promising emerging approach for preventing and/or treating UC. Natural products provide substantial opportunities for the discovery and development of anti-inflammatory drugs[5]. A variety of natural chemicals, drugs, and extracts have the potential to treat UC by regulating macrophage polarization[24,25]. For instance, dioscin, a steroidal saponin derived from *Dioscorea nipponica* Makino, can alleviate UC by inhibiting M1 macrophage polarization and promoting M2 macrophage polarization [7]. The underlying mechanisms of dioscin in such regulation of macrophage polarization are possibly the inhibition of the mammalian target of rapamycin complex 1 (mTORC1)/hypoxia-inducible factor-1α (HIF-1α) signaling pathway in M1 macrophages and the promotion of the mammalian target of rapamycin complex 2 (mTORC2)/peroxisome proliferator-activated receptor γ (PPARγ) signals in M2 macrophages [7]. Moreover, tiliroside is a natural flavonoid that exists widely in plants. Tiliroside can ameliorate UC by converting M1 macrophages into M2 macrophages via downregulation of the HIF-1α/glycolysis pathway [26]. Furthermore, a well-known traditional Chinese formula, Huangqin decoction, has been demonstrated to have protective effects against UC by regulating macrophage polarization through the activation of the free fatty acid receptor 4 (FFAR4)/PPARα signaling pathway[27]. These findings demonstrate the potential application of natural products for the treatment of UC via the regulation of macrophage polarization. In the present study, we found that AR extract can convert M1 macrophages into M2 macrophages then reduce the protein and mRNA expression of pro-inflammatory cytokines, including iNOS, TNF-α, IL-6, IL-1β, and NO, and enhance the mRNA expression of M2 macrophages, including CD206, Arg-1, Fizz-1, and Ym-1, in RAW 264.7 cells. In our DSS-induced UC mouse model, AR also promoted M2 macrophage polarization and suppressed M1 macrophage polarization. AR significantly increased the number of CD206-positive macrophages and upregulated Arg-1 protein expression, while decreasing both the number of CD86-positive macrophages and iNOS expression. These findings

suggest that AR is a potential treatment for UC via the regulation of macrophage polarization.

The MAPK signaling pathway plays an important role in the pathogenesis of UC. Specifically, the MAPK signaling pathway is a key extracellular signal transduction pathway that is triggered by oxidative stress, growth factors, pro-inflammatory mediators, and pathogen-associated molecular patterns. The pathway then initiates the activation of the transcription factors C-Fos and C-Jun by activating p38, ERK, and JNK cascades[28,29]. Subsequently, these transcription factors can translocate into the nucleus and control the transcription of pro-inflammatory factors, such as IL-6, TNF-α, and IL-1β[30]. Ultimately, this process leads to intestinal inflammation and the onset of UC. There are three components of the MAPK pathway: the ERK, JNK, and p38 signaling pathways[31]. The ERK pathway regulates cell differentiation and growth, while the p38 and JNK pathways play crucial roles in stress response processes like cell apoptosis and inflammation[32]. Previous studies showed that MAPK pathways, including the ERK, JNK, and p38 signaling pathways, were significantly activated in the colon tissues of animals with UC[33,34]. Blocking the MAPK pathway and its downstream signaling in patients with UC can significantly reduce intestinal inflammation, delay disease progression, and provide insights for the development of potential anti-UC drugs[35]. A recent study reported that shikimic acid, an anti-inflammatory compound derived from anise, can ameliorate DSS-induced UC in mice by reversing weight loss, decreasing DAI scores, enhancing the intestinal barrier, and reducing the destruction of colonic structure[36]. The investigators also found that shikimic acid can suppress the inflammation response in the colon tissues of UC mice by reducing the levels of TNF-α and IL-1β, and the underlying anti-inflammatory and anti-UC mechanisms of shikimic acid are likely through the inhibition of ERK, JNK, and p38 MAPK signal transduction[36]. Similar results were found in studies of the anti-UC effects of anemoside B4[37], Shaoyao decoction[38], and andrographolide[39]. Therefore, suppressing MAPK signal transduction could be a potential strategy for treating UC. In the present study, we demonstrated that MAPK signals, including MEK1/2, ERK1/2, JNK1/2, and p38, were activated in RAW 264.7 macrophages in response to LPS treatment, which is consistent with previous studies. Additionally, we showed that LPS-induced phosphorylation of MEK1/2, ERK1/2, JNK1/2, and p38 was significantly suppressed by AR extract, particularly at 1 mg/mL and 2 mg/mL. These results suggest that the underlying anti-UC mechanisms of AR could be the downregulation of MAPK signaling pathways.

Nod-like receptor protein 3 (NLRP3) inflammasome is believed to be another critical mechanism in the pathogenesis of UC. NLRP3 is a protein complex composed of multiple proteins that mediate the assembly of inflammasome complexes in the presence of microbial ligands, leading to the activation of cysteine aspartate protease-1 (caspase-1) and secretion of pro-inflammatory cytokines (e.g. IL-1β and IL-18), thereby stimulating the inflammatory response [40]. Therefore, targeting NLRP3 inflammasome and its downstream signal caspase-1 could be considered as the promising strategy for the treatment of UC [41]. Accumulating evidence suggests that ROS are likely the upstream mediators that regulate the development of NLRP3-associated UC. For instance, Zhong et al. reported that particulate stimuli could induce ROS production in mitochondria, and further trigger calcium influx through transient receptor potential melastatin 2 (TRPM2), resulting in the activation of NLRP3 inflammasome [42]. The activators of NLRP3 inflammasome can trigger the release of ROS and further induce oxidative stress injury on colon epithelial cells. Similarly, inhibition of ROS production can also block the activity of NLRP3. Apparently, DSS can induce the oxidative stress along with the activation of NLRP3 during UC development [43]. In the present study, we showed that AR can suppress DSS-induced inflammation and ROS production in Caco-2 cells and mouse colon tissues. Based on the results of our network pharmacology analysis, NLRP3 is also closely involved in the regulation of AR-induced protective effects against UC. Although there is no solid evidence in the present study shows that the blockade of NLRP3 may possibly contribute to the anti-UC effects of AR, the role of NLRP3 in AR-induced protective effects against UC is still worth investigating in the future.

Accumulating evidence has demonstrated that DSS-induced UC is a relatively mature model that produces symptoms similar to those of UC patients, including weight loss, diarrhea, and even hematochezia[44,45]. Therefore, this animal model is frequently used to simulate the pathogenesis of UC and screen for anti-UC drugs[46]. In addition, oxidative stress is another major cause of colon damage during the pathogenesis of UC[47]. One of the key features of this experimentally induced colitis is tissue damage caused by oxidative stress[46]. Consistent with this, we found that DSS can cause significant oxidative stress and colon damage in mice. DSS increased the level of MDA and reduced the levels of SOD, GSH, and CAT in the colon tissues of mice. In contrast, AR extract significantly suppressed oxidative stress by reducing ROS production and MDA release and by restoring levels of SOD, GSH, and CAT in the colons of DSS-treated mice. Additionally, DSS induced abundant ROS generation and mitochondrial dysfunction in Caco-2 cells. We previously demonstrated that AR extract has remarkable antioxidant capacities in PC12 rat pheochromocytoma, leading to protection against 6-OHDA-induced oxidative damage in PC12 cells [14]. Similarly, in the present study, we showed that DSS-induced ROS generation and mitochondrial respiratory dysfunction in Caco-2 cells were strongly suppressed by AR extract, demonstrating the substantial anti-oxidative effects of AR. These findings suggest that the protective effects of AR against DSS-induced colon damage are likely due to its remarkable antioxidant capacity.

Although CD86 is considered as the primary surface biomarker of M1 macrophages, recent studies have indicated that it is also found on the surface of M2b macrophages [48]. As one of the subtypes of M2 macrophages, M2b macrophages showed different functional roles compared with other M2 macrophages. M2b macrophages are also known as regulatory macrophages, and they can be induced by the combination of immune complex and toll-like receptor agonists [49]. They play a vital role in stimulating pro-inflammatory response by releasing a high level of IL-1β, IL-6, and TNF-α. Therefore, M2b macrophages are closely implicated with infectious diseases, autoimmune disease, and cardiovascular diseases [49]. However, a recent study reported that DSS can induce the M2b macrophages polarization *in vitro* by increasing the mRNA expressions of specific biomarkers of M2b macrophages, including SPHK1 and LIGHT [50]. This evidence reveals that M2b macrophages may also be activated by DSS in animals. Therefore, it is reasonable to suspect that the population of $CD86^{+}$ macrophages shown in this study may consist of M1 macrophages and M2b macrophages. Although there are limited studies reported the polarization of M2b macrophages in response to DSS treatment, this data warrants further investigation. Herein, we still recommend the use of as many biomarkers as possible to identify M1 macrophages in UC animal models, rather than using only the CD86 antibody.

5. Conclusion

In conclusion, we demonstrated that AR extract can protect against DSS-induced UC by regulating macrophage polarization and suppressing oxidative stress. The underlying anti-UC mechanism of AR is likely through the downregulation of MAPK signaling pathways. These valuable findings suggest that adequate intake of AR can prevent and/or treat UC and can also provide insights for the future development of anti-UC drugs or supplements derived from this edible mushroom.

CRediT authorship contribution statement

Jingjing Li: Writing – original draft, Visualization, Investigation, Funding acquisition, Formal analysis. **Chaomei Fu:** Project administration. **Sai-wang Seto:** Writing – review & editing, Supervision, Data

curation. **Xi Luo:** Methodology, Investigation, Formal analysis. **Polly Ho-Ting Shiu:** Methodology, Investigation, Formal analysis. **Jinming Zhang:** Writing – review & editing, Supervision, Data curation, Conceptualization. **Chengwen Zheng:** Methodology. **Xuebo Li:** Methodology. **Renkai Li:** Methodology. **Simon Ming-Yuen Lee:** Writing – review & editing. **George Pak-Heng Leung:** Writing – review & editing, Supervision, Data curation, Conceptualization. **Yanfen Cheng:** Formal analysis. **Xin Nie:** Methodology. **Panthakarn Rangsinth:** Methodology. **Benson Wui Man Lau:** Methodology, Formal analysis.

Declaration of Competing Interest

The authors declare that they have no known competing financial interests or personal relationships that could have appeared to influence the work reported in this paper.

Data availability

Data will be made available on request.

Acknowledgments

This study was supported by Shenzhen Science and Technology Program (Grant no. JCYJ20230807140259002), Guangdong Basic and Applied Basic Research Foundation (Grant no. 2023A1515011960), Start-up Fund for research assistant professors under the Strategic Hiring Scheme (Grant no. A0040914), and Seed Fund from Research Centre for Chinese Medicine Innovation (Grant no. P0045264), Hong Kong Polytechnic University, Hung Hom, Kowloon, Hong Kong SAR, P.R. China. This study was also supported by CDUTCM Undergraduate Innovation and Entrepreneurship Training Program (Grant no. 202310633035).

Consent for publication

All authors have provided their consent for publication of the manuscript.

Appendix A. Supporting information

Supplementary data associated with this article can be found in the online version at doi:10.1016/j.biopha.2024.116901.

References

1 R. Shivashankar, et al., Incidence and Prevalence of Crohn's Disease and Ulcerative Colitis in Olmsted County, Minnesota From 1970 Through 2010, Clin. Gastroenterol. Hepatol. 15 (6) (2017) 857–863.
2 L. Du, C. Ha, Epidemiology and Pathogenesis of Ulcerative Colitis, Gastroenterol. Clin. North Am. 49 (4) (2020) 643–654.
3 C. Zhang, et al., Oral colon-targeting core-shell microparticles loading curcumin for enhanced ulcerative colitis alleviating efficacy, Chin. Med. 16 (1) (2021) 92.
4 W.J. Sandborn, et al., Ozanimod as Induction and Maintenance Therapy for Ulcerative Colitis, N. Engl. J. Med. 385 (14) (2021) 1280–1291.
5 K. Wang, et al., A potential therapeutic approach for ulcerative colitis: targeted regulation of macrophage polarization through phytochemicals, Front. Immunol. 14 (2023) 1155077.
6 A.J. Boutilier, S.F. Elsawa, Macrophage Polarization States in the Tumor Microenvironment, Int. J. Mol. Sci. 22 (13) (2021).
7 M.M. Wu, et al., Dioscin ameliorates murine ulcerative colitis by regulating macrophage polarization, Pharmacol. Res. 172 (2021) 105796.
8 W. Cheng, et al., Huanglian-Houpo extract attenuates DSS-induced UC mice by protecting intestinal mucosal barrier and regulating macrophage polarization, J. Ethnopharmacol. 307 (2023) 116181.
9 T. Sun, et al., Amelioration of ulcerative colitis via inflammatory regulation by macrophage-biomimetic nanomedicine, Theranostics 10 (22) (2020) 10106–10119.
10 X. Luo, et al., Advances and Prospects of Prolamine Corn Protein Zein as Promising Multifunctional Drug Delivery System for Cancer Treatment, Int. J. Nanomed. 18 (2023) 2589–2621.
11 M. Zhang, et al., Roles of macrophages on ulcerative colitis and colitis-associated colorectal cancer, Front. Immunol. 14 (2023) 1103617.
12 Z. Yang, et al., A potential therapeutic target in traditional Chinese medicine for ulcerative colitis: Macrophage polarization, Front. Pharmacol. 13 (2022) 999179.
13 C.W. Zheng, T.M. Cheung, G.P. Leung, A review of the phytochemical and pharmacological properties of Amauroderma rugosum, Kaohsiung J. Med. Sci. 38 (6) (2022) 509–516.
14 J. Li, et al., Amauroderma rugosum Protects PC12 Cells against 6-OHDA-Induced Neurotoxicity through Antioxidant and Antiapoptotic Effects, Oxid. Med. Cell Longev. 2021 (2021) 6683270.
15 P.M. Chan, et al., Attenuation of Inflammatory Mediators (TNF-alpha and Nitric Oxide) and Up-Regulation of IL-10 by Wild and Domesticated Basidiocarps of Amauroderma rugosum (Blume & T. Nees) Torrend in LPS-Stimulated RAW264.7 Cells, PLoS One 10 (10) (2015) e0139593.
16 P.M. Chan, et al., Amauroderma rugosum (Blume & T. Nees) Torrend: Nutritional Composition and Antioxidant and Potential Anti-Inflammatory Properties, Evid. Based Complement Alternat Med. 2013 (2013) 304713.
17 P.H. Shiu, et al., Amauroderma rugosum Extract Suppresses Inflammatory Responses in Tumor Necrosis Factor Alpha/Interferon Gamma-Induced HaCaT Keratinocytes, Molecules 27 (19) (2022).
18 G. Jena, P.P. Trivedi, B. Sandala, Oxidative stress in ulcerative colitis: an old concept but a new concern, Free Radic. Res. 46 (11) (2012) 1339–1345.
19 Y.C. Liu, et al., Macrophage polarization in inflammatory diseases, Int. J. Biol. Sci. 10 (5) (2014) 520–529.
20 A.J. Petty, Y. Yang, Tumor-associated macrophages: implications in cancer immunotherapy, Immunotherapy 9 (3) (2017) 289–302.
21 Y. Cheng, et al., Glycyrrhetinic acid suppresses breast cancer metastasis by inhibiting M2-like macrophage polarization via activating JNK1/2 signaling, Phytomedicine 114 (2023) 154757.
22 Nie, X., et al., Garcinone E suppresses breast cancer growth and metastasis by modulating tumor-associated macrophages polarization via STAT6 signaling. Phytother Res, 2023.
23 T.C. DeRoche, S.Y. Xiao, X. Liu, Histological evaluation in ulcerative colitis, Gastroenterol. Rep. (Oxf.) 2 (3) (2014) 178–192.
24 X. Wang, et al., Oral administration of Huanglian-Houpo herbal nanoemulsion loading multiple phytochemicals for ulcerative colitis therapy in mice, Drug Deliv. 30 (1) (2023) 2204207.
25 X. Zhang, et al., Chinese herbal medicines in the treatment of ulcerative colitis: a review, Chin. Med 17 (1) (2022) 43.
26 H. Zhuang, et al., Tiliroside Ameliorates Ulcerative Colitis by Restoring the M1/M2 Macrophage Balance via the HIF-1alpha/glycolysis Pathway, Front. Immunol. 12 (2021) 649463.
27 M.Y. Li, et al., Huangqin Decoction ameliorates ulcerative colitis by regulating fatty acid metabolism to mediate macrophage polarization via activating FFAR4-AMPK-PPARalpha pathway, J. Ethnopharmacol. 311 (2023) 116430.
28 O.J. Broom, et al., Mitogen activated protein kinases: a role in inflammatory bowel disease? Clin. Exp. Immunol. 158 (3) (2009) 272–280.
29 Z.Y. Liu, et al., The new andrographolide derivative AGS-30 induces apoptosis in human colon cancer cells by activating a ROS-dependent JNK signalling pathway, Phytomedicine 94 (2022).
30 J.M. Kyriakis, J. Avruch, Mammalian MAPK signal transduction pathways activated by stress and inflammation: a 10-year update, Physiol. Rev. 92 (2) (2012) 689–737.
31 E.K. Kim, E.J. Choi, Compromised MAPK signaling in human diseases: an update, Arch. Toxicol. 89 (6) (2015) 867–882.
32 U. Moens, S. Kostenko, B. Sveinbjornsson, The Role of Mitogen-Activated Protein Kinase-Activated Protein Kinases (MAPKAPKs) in Inflammation, Genes (Basel) 4 (2) (2013) 101–133.
33 X. Zhao, et al., Evaluation of p38 MAPK pathway as a molecular signature in ulcerative colitis, J. Proteome Res 10 (5) (2011) 2216–2225.
34 M. Zhou, et al., Boosting mTOR-dependent autophagy via upstream TLR4-MyD88-MAPK signalling and downstream NF-kappaB pathway quenches intestinal inflammation and oxidative stress injury. EBioMedicine 35 (2018) 345–360.
35 J. Zhang, et al., Macrophage-based nanotherapeutic strategies in ulcerative colitis, J. Control Release 320 (2020) 363–380.
36 X. Li, et al., Shikimic Acid Regulates the NF-kappaB/MAPK Signaling Pathway and Gut Microbiota to Ameliorate DSS-Induced Ulcerative Colitis. J. Agric. Food Chem. 71 (23) (2023) 8906–8914.
37 H. Ma, et al., Anemoside B4 prevents acute ulcerative colitis through inhibiting of TLR4/NF-kappaB/MAPK signaling pathway, Int Immunopharmacol. 87 (2020) 106794.
38 Y.Y. Wei, et al., Shaoyao decoction attenuates DSS-induced ulcerative colitis, macrophage and NLRP3 inflammasome activation through the MKP1/NF-kappaB pathway, Phytomedicine 92 (2021) 153743.
39 Z. Gao, et al., Andrographolide derivative CX-10 ameliorates dextran sulphate sodium-induced ulcerative colitis in mice: Involvement of NF-kappaB and MAPK signalling pathways, Int Immunopharmacol. 57 (2018) 82–90.
40 F.S. Sutterwala, et al., Critical role for NALP3/CIAS1/cryopyrin in innate and adaptive immunity through its regulation of caspase-1, Immunity 24 (3) (2006) 317–327.
41 Y. Zhen, H. Zhang, NLRP3 Inflammasome and Inflammatory Bowel Disease, Front Immunol. 10 (2019) 276.
42 Z. Zhong, et al., TRPM2 links oxidative stress to NLRP3 inflammasome activation, Nat. Commun. 4 (2013) 1611.
43 C. Bauer, et al., Colitis induced in mice with dextran sulfate sodium (DSS) is mediated by the NLRP3 inflammasome, Gut 59 (9) (2010) 1192–1199.
44 L. Pang, et al., Protective role of ergothioneine isolated from Pleurotus ostreatus against dextran sulfate sodium-induced ulcerative colitis in rat model, J. Food Sci. 87 (1) (2022) 415–426.

45 J. Xian, et al., Colonic Delivery of Celastrol-Loaded Layer-by-Layer Liposomes with Pectin/Trimethylated Chitosan Coating to Enhance Its Anti-Ulcerative Colitis Effects, Pharmaceutics 13 (12) (2021).
46 X. Wang, et al., Oral Core-Shell Nanoparticles Embedded in Hydrogel Microspheres for the Efficient Site-Specific Delivery of Magnolol and Enhanced Antiulcerative Colitis Therapy, ACS Appl. Mater. Interfaces 13 (29) (2021) 33948–33961.
47 B.L. Xu, G.J. Zhang, Y.B. Ji, Active components alignment of Gegenqinlian decoction protects ulcerative colitis by attenuating inflammatory and oxidative stress, J. Ethnopharmacol. 162 (2015) 253–260.
48 B. Zhang, et al., Age decreases macrophage IL-10 expression: Implications for functional recovery and tissue repair in spinal cord injury, Exp. Neurol. 273 (2015) 83–91.
49 L.X. Wang, et al., M2b macrophage polarization and its roles in diseases, J. Leukoc. Biol. 106 (2) (2019) 345–358.
50 Y. Kono, S. Miyoshi, T. Fujita, Dextran sodium sulfate alters cytokine production in macrophages in vitro, Pharmazie 71 (11) (2016) 619–624.